Electronic Supplementary Information

Spectroscopic study of the excited state proton transfer processes of (8-bromo-7-hydroxyquinolin-2-yl)methyl-protected phenol in aqueous solutions

Jinqing Huang,[a,‡] Adna Muliawan,[b,‡] Jiani Ma,*[c] Ming De Li,[a] Hoi Kei Chiu,[a] Xin Lan,[a] Davide Deodato,[b] David Lee Phillips,*[,a] and Timothy M. Dore*[,b,d]

[a] *Department of Chemistry, The University of Hong Kong, Pokfulam Road, Hong Kong, People's Republic of China*

[b] *New York University Abu Dhabi, P.O. Box 129188, Abu Dhabi, United Arab Emirates*

[c] *Key Laboratory of Synthetic and Natural Functional Molecule Chemistry of Ministry of Education, College of Chemistry and Materials Science, Northwest University, Xi'an, People's Republic of China.*

[d] *Department of Chemistry, University of Georgia, Athens, GA 30602, USA*

[‡] *These authors contributed equally to this work.*

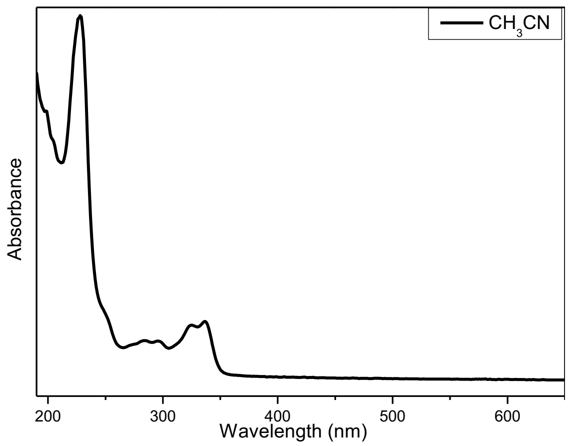

Figure S1. UV-Vis absorption spectrum of BHQ-OPh in acetonitrile.

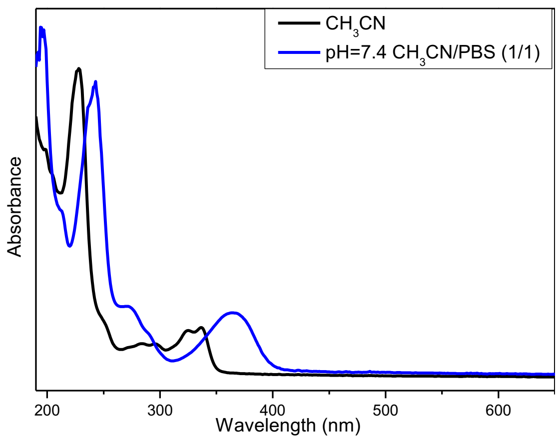

Figure S2. UV-Vis absorption spectra of BHQ-OPh in acetonitrile and 1:1 acetonitrile/PBS (pH 7.4).

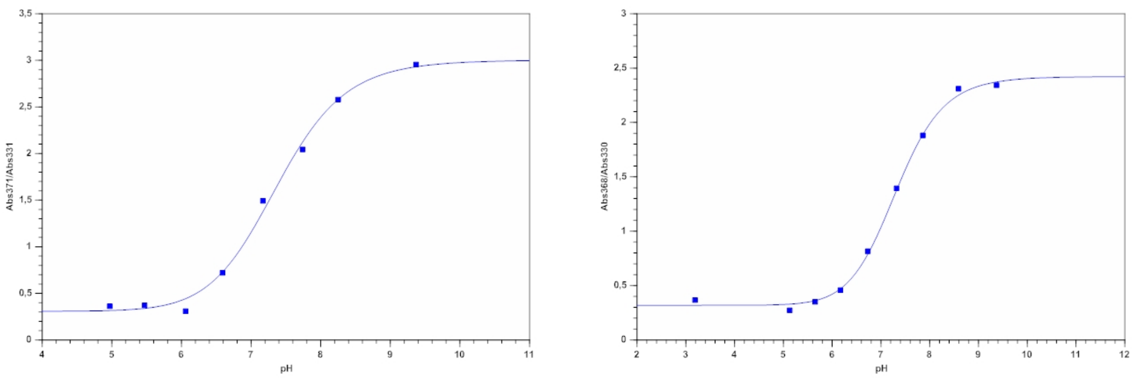

Figure S3. Titration of BHQ-OPh (left) and BHQ-OAc (right) to determine the pK_a of the phenolic proton. BHQ-OPh or BHQ-OAc was dissolved in buffers of known pH, and its spectral maxima were noted by UV-vis at 331 (phenol) and 371 nm (phenolate) (or 330 and 368 nm for BHQ-OAc). The ratio of the absorbance at the two reference wavelengths was plotted vs pH of the buffer. The plot is fitted with a sigmoidal regression and the pK_a was calculated by solving for the inflection point. Buffers (pH): phosphate (3.91, 6.73, 7.32, and 7.86), acetate (5.13 and 5.65), citrate (6.17), borate (8.59 and 9.47).

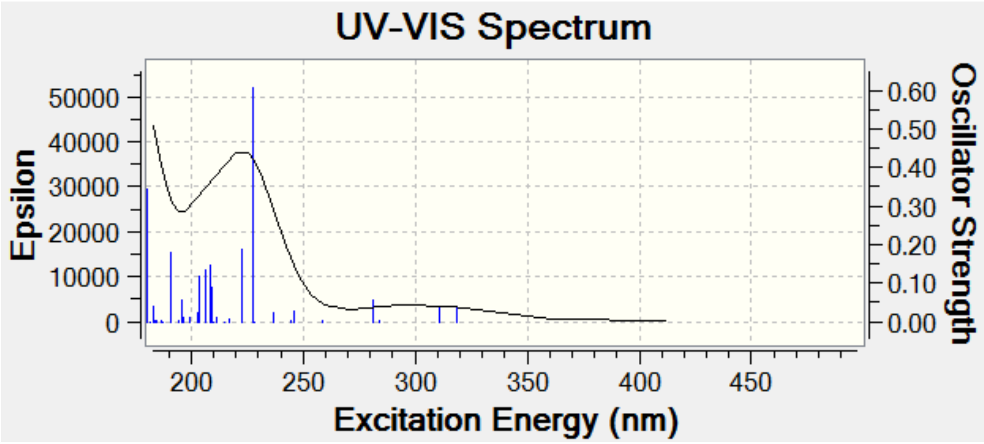

Figure S4. Simulated absorption spectrum of BHQ-OPh (N) obtained from TD-DFT calculation at the level of B3LYP/6-311G**.

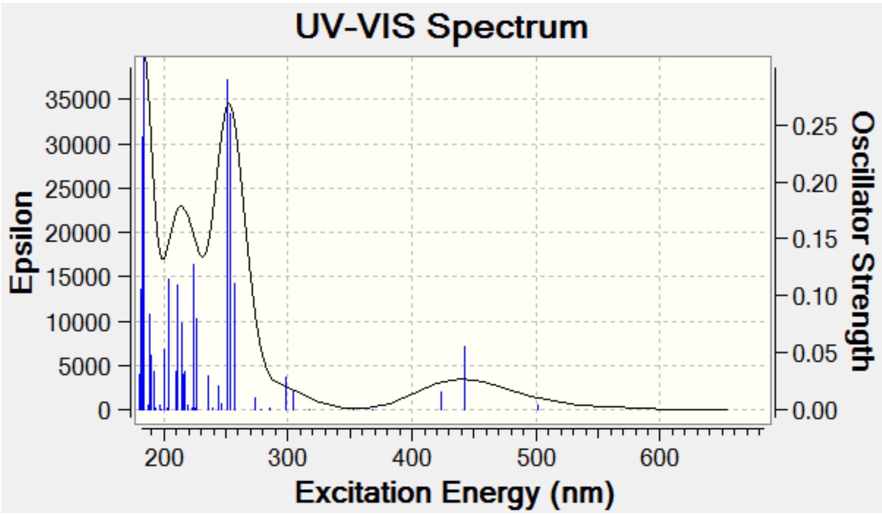

Figure S5. Simulated absorption spectrum of BHQ-OPh (A) obtained from TD-DFT calculation at the level of B3LYP/6-311G**

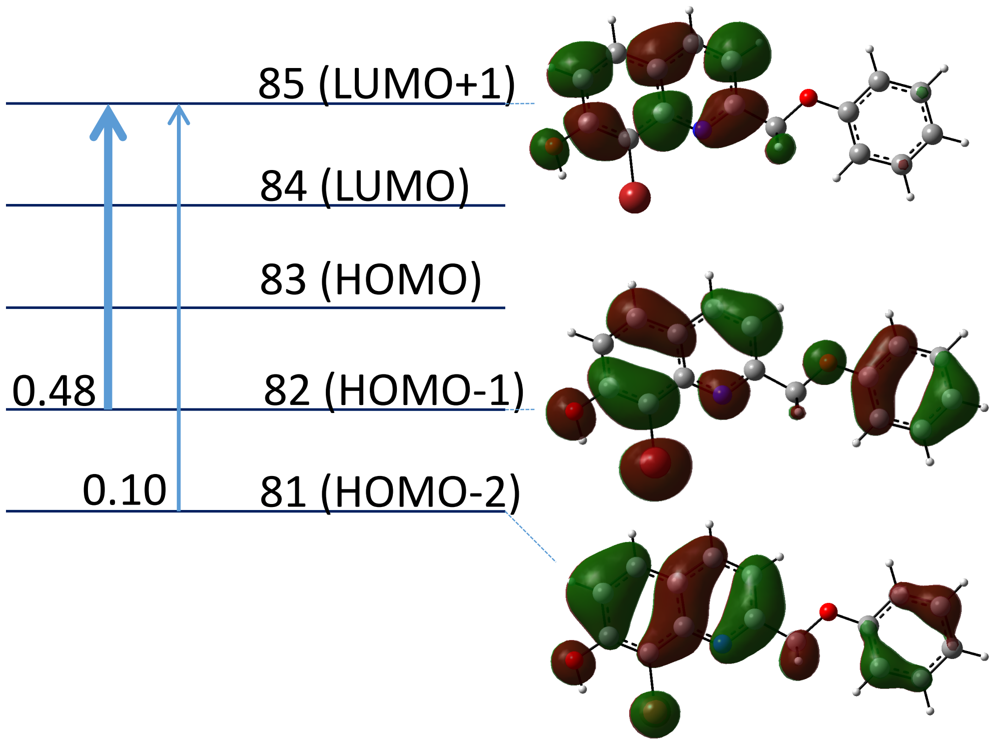

Figure S6. Frontier molecular orbitals of the strongest oscillator strength transition at 227.78 nm for BHQ-OPh (N).

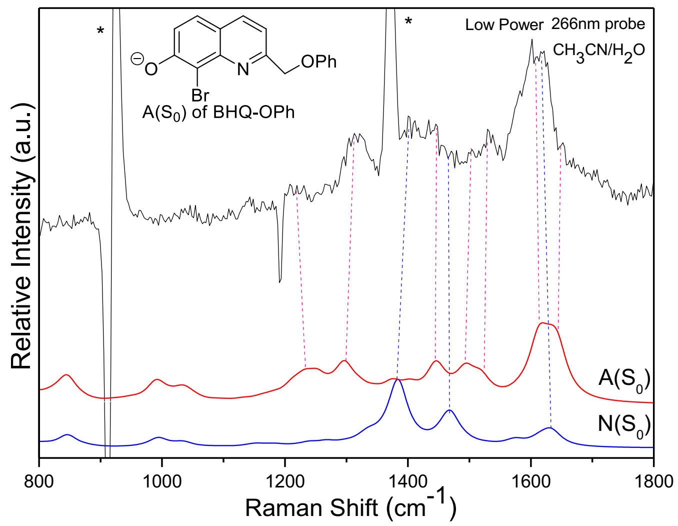

Figure S7. Comparison between low power 266-nm resonance Raman spectrum of BHQ-OPh in 1:1 acetonitrile/water and the DFT calculated Raman spectra of $N(S_0)$ and $A(S_0)$ of BHQ-OPh.

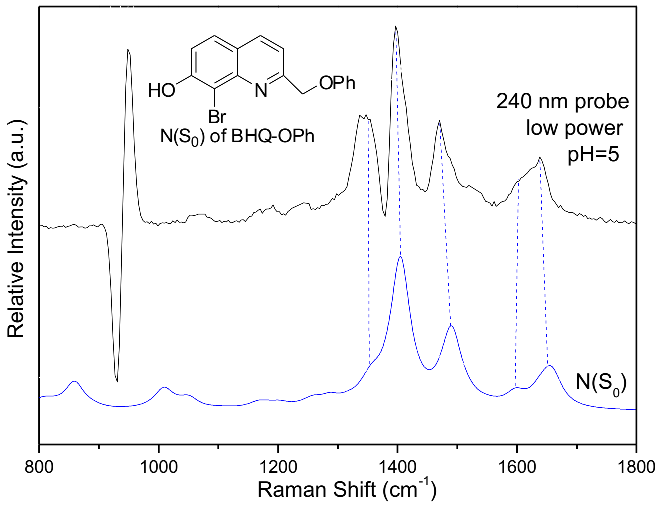

Figure S8. Comparison between low power 240-nm resonance Raman spectrum of BHQ-OPh in 1:1 acetonitrile/water (pH 5) solution and the DFT calculated Raman spectrum of $N(S_0)$ of BHQ-OPh.

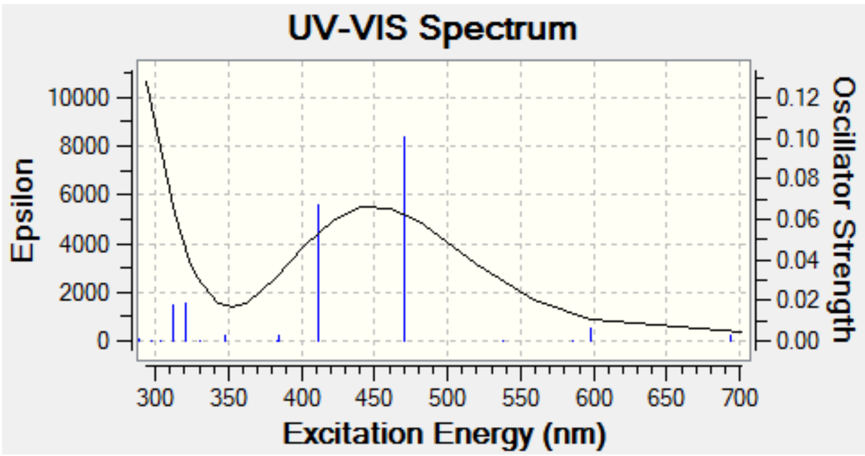

Figure S9. Simulated absorption spectrum for the T_1 state of BHQ-OPh (N) obtained from TD-DFT calculation at the level of B3LYP/6-311G**

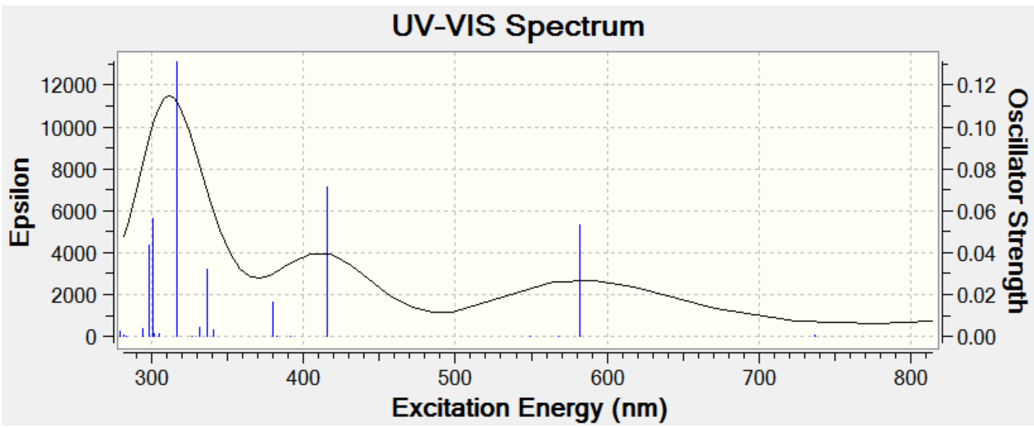

Figure S10. Simulated absorption spectrum for the T_1 state of BHQ-OPh (A) obtained from TD-DFT calculation at the level of B3LYP/6-311G**

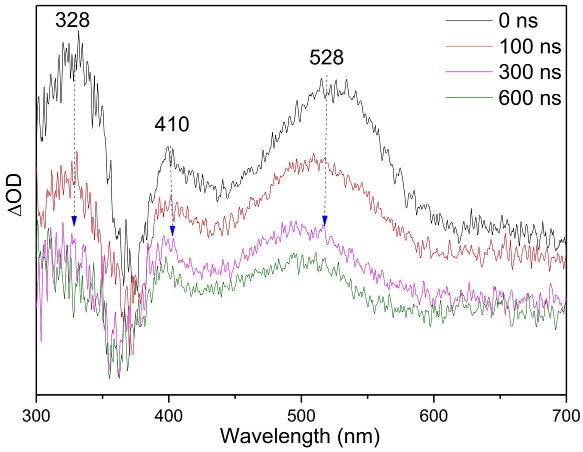

Figure S11. ns-TA spectra of BHQ-OPh in PBS (pH 7.4) after 266-nm excitation.

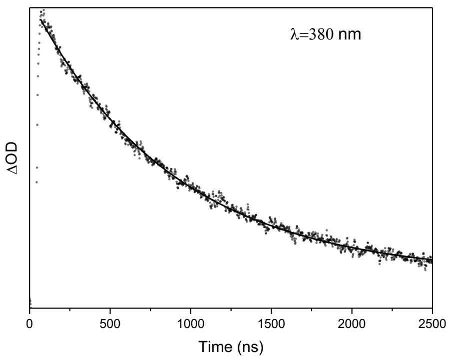

Curve fit:

$$y = y_0 + A_1 e^{-(x-x_0)/t_1}$$

$y_0 = 0.007030$

$x_0 = 51.73233$

$A_1 = 0.056530$

$t_1 = 874.97694$

Figure S12. Fit of the ns-TA spectra in Fig. 4c to determine the rate constant for the decay of the T_1 state of BHQ-OPh (T).

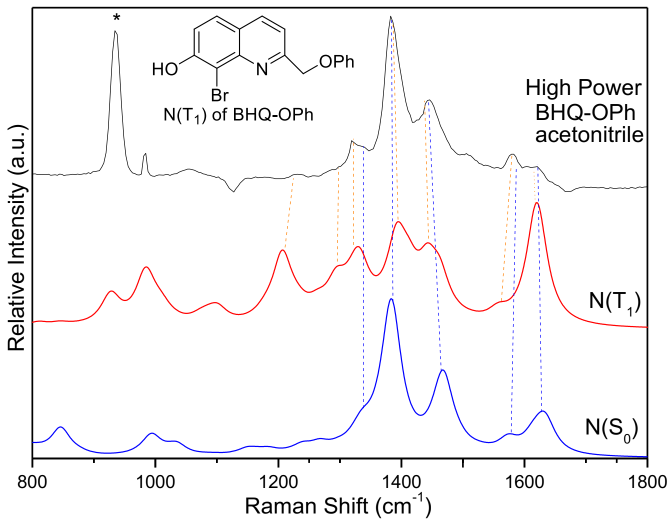

Figure S13. Comparison between high power 240-nm resonance Raman spectrum of BHQ-OPh in acetonitrile and the DFT calculated Raman spectra of the T_1 and S_0 states of BHQ-OPh (N).

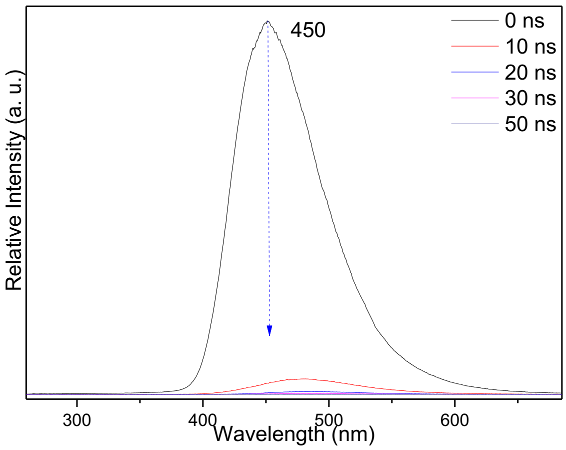

Figure S14. ns-EM spectra of BHQ-OPh in PBS (pH 7.4) after 266-nm excitation.

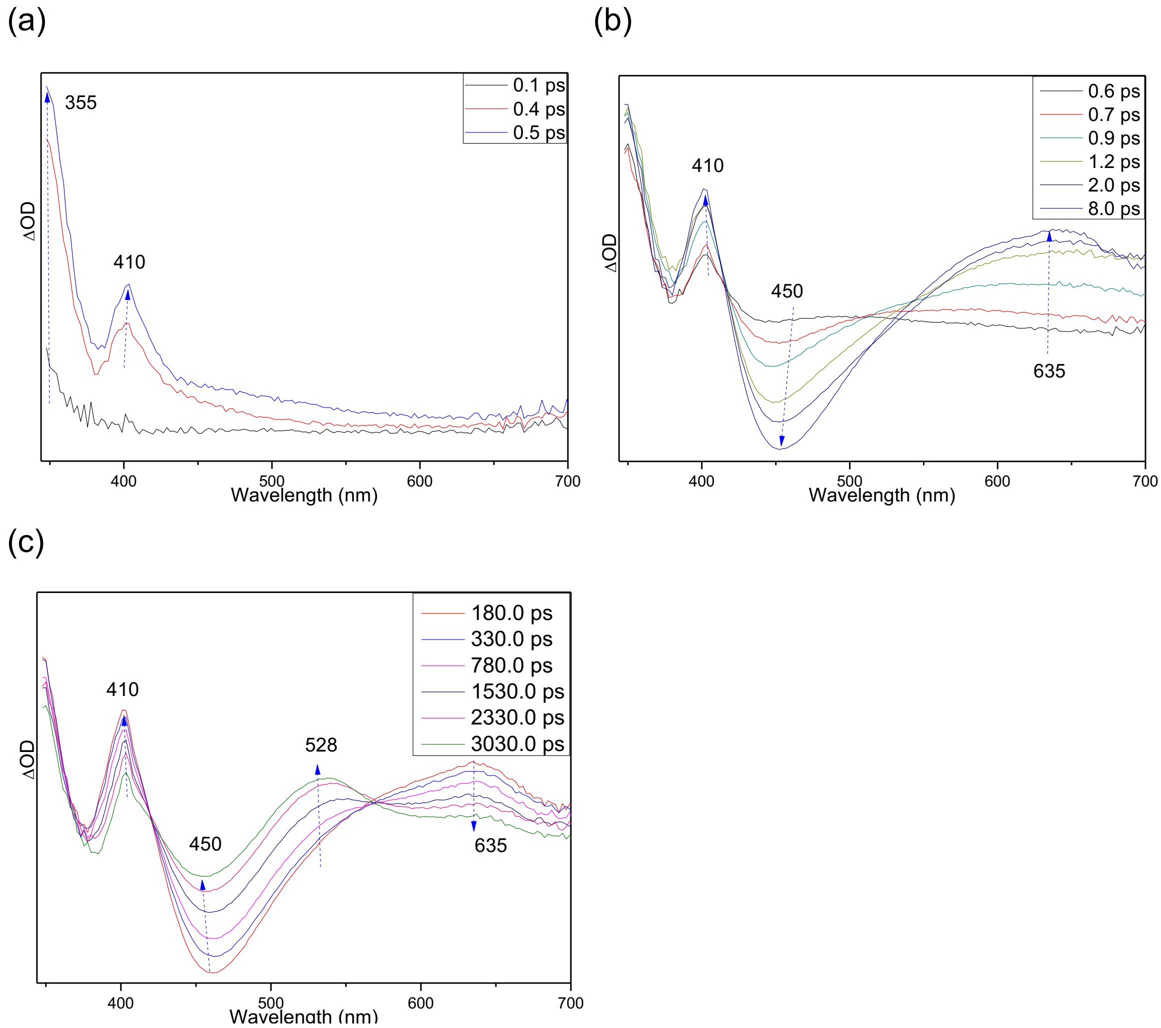

Figure S15. fs-TA spectra of BHQ-OPh in 1:1 acetonitrile/PBS (pH 7.4) after 266-nm excitation. (a) The growth of the 355-nm absorption band within 1 ps results from excitation from the ground state BHQ-OPh (A). (b) Subsequently, there is a conversion with an emission band at 450 nm and an absorption band at 635 nm. Based on the assignments for the ns-EM spectra in 1:1 acetonitrile/PBS (pH 7.4) (Fig. 7), the emission band at 450 nm is attributed to the fluorescence from the S_1 state of BHQ-OPh (A). Hence, the conversion in (b) can be assigned to the formation of the S_1 state of BHQ-OPh (A). (c) The growing features at 410 and 528 nm are assigned to the T_1 state of BHQ-OPh (A) based on the ns-TA spectra (Fig. 4). The conversion in (c) indicates the intersystem crossing from the S_1 state of BHQ-OPh (A) to the T_1 state of BHQ-OPh (A).

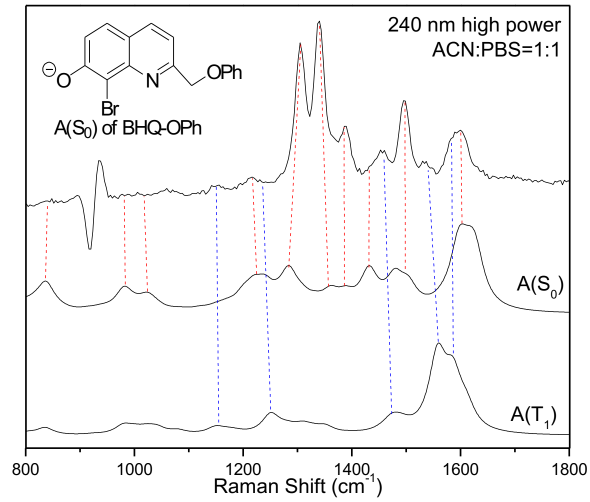

Figure S16. Comparison between the high power 240-nm resonance Raman spectrum of BHQ-OPh in 1:1 acetonitrile/PBS (pH 7.4) and the DFT calculated Raman spectra of the T_1 and S_0 states of BHQ-OPh (A).

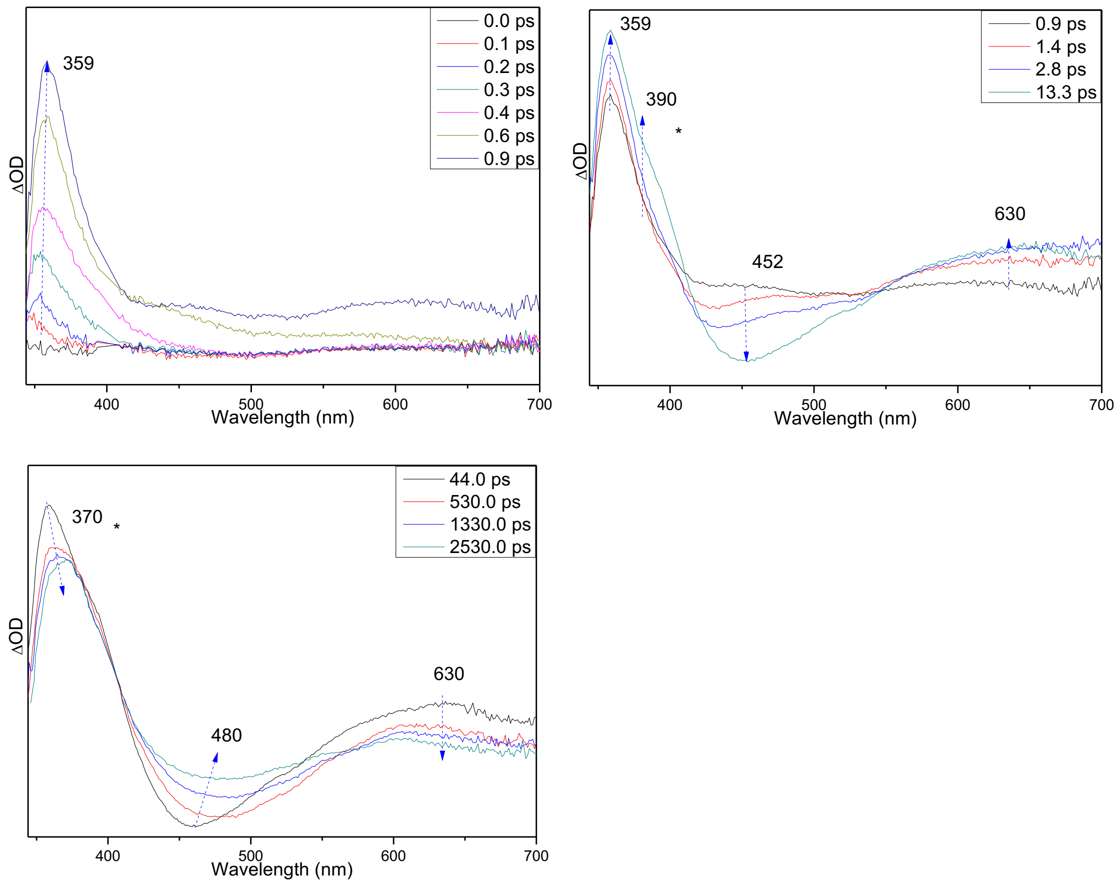

Figure S17. fs-TA spectra of BHQ-OPh in 1:1 acetonitrile/water (pH 5.0) after 266-nm excitation.

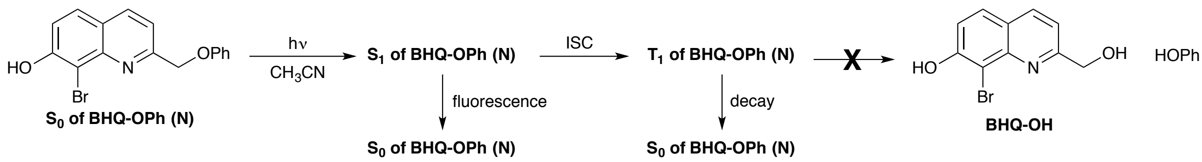

Scheme S1. Proposed mechanism of BHQ-OPh photoprocesses in acetonitrile.

Table S1. Selected electronic transition energies, oscillator strength in the region of 210-310 nm, and molecular orbital transitions for the strongest oscillator strength transition at 227.78 nm obtained from (U)B3LYP/6−311G** TD−DFT calculations for the neutral form of BHQ-OPh.

Neutral Form			
Excitation Energy (nm)	Oscillator Strength	Molecular Orbital Transitions for 227.78 excitation	
211.42	0.0099		
216.88	0.0002	78 -> 84	-0.25951
217.12	0.0043	78 -> 85	-0.12958
222.38	0.1865	81 -> 84	-0.27312
227.78	**0.6085**	81 -> 85	0.10130
228.02	0.0001	81 -> 88	-0.11514
236.93	0.0227	82 -> 85	0.47862
244.56	0.0002	83 -> 85	-0.20895
245.78	0.0262		
258.94	0.0031		
281.48	0.0549		
283.71	0.0013		